Electronic Supplementary Material (ESI) for Journal of Materials Chemistry A.

A low cost azomethine-based hole transporting material for perovskite photovoltaics

Michiel L. Petrus,[a,b] Thomas Bein,[a] Theo J. Dingemans,[b] and Pablo Docampo[a]

[a] Department of Chemistry, University of Munich (LMU), Butenandtstrasse 5-13, 81377 Munich, Germany
[b] Delft University of Technology, Faculty of Aerospace Engineering, Kluyverweg 1, 2629 HS Deft, The Netherlands.

Table of Contents

Experimental

All chemicals were purchased from commercial sources and used as received unless stated otherwise.

The structures were confirmed by ^{1}H-NMR (Bruker WM-400, 400 MHz) and ^{13}C-NMR (Bruker WM-400, 100 MHz). All samples were dissolved in deuterated solvents and the recorded spectra were referenced to the solvent ($CDCl_3$: ^{1}H, 7.26 and ^{13}C 77.0 ppm C_6D_6: 7.36 ppm) relative to TMS. Infrared spectra were obtained with a PerkinElmer Spectrum 100 and UV-vis spectra were collected using a PerkinElmer Lambda 35 UV-vis spectrometer. GC-MS analyses were performed on a Shimadzu GC2010 series GC coupled to a MS detector (Shimadzu QP2010S) and equipped with a BPX5 capillary column. The oven was heated from 50–300 °C at a rate of 10 °C min^{-1} using a 1 mL min^{-1} helium gas flow. The sample was injected using an Atas GL Optic 3 inlet which was heated from 50–300 °C in one minute. Mass spectra were generated by electron impact and data was collected over the *m/z* range 45–900. Mass spectra were recorded using a Shimadzu QP2010S with direct injection port.

Electrochemical measurements

Cyclic voltammetry (CV) experiments were performed using a Metrohm Potentiostat (PGSTAT302N) with platinum working and counter electrode and an Ag/AgCl reference electrode. Experiments were performed in anhydrous and degassed dichloromethane solutions of the hole transporter with 0.1 M tetrabutylammonium hexafluorophosphate (*t*BuNPF$_6$) as electrolyte and a scan rate of 100 mV s^{-1}. HOMO levels have been calculate according to literature (the formal potential of the Fc^+/Fc redox couple used is −5.1 eV).[1]

Thermal and calorimetric analysis

Thermogravic analysis (TGA) was performed on a Perkin Elmer Pyris diamond TG/DTA under a nitrogen atmosphere with a heating rate of 10 °C min^{-1}. Differential scanning calorimetry (DSC) was performed on a Perkin Elmer Sapphire DSC using a heating rate of 20 °C min^{-1}. Melting behaviour was confirmed by optical microscopy using a hot stage.

Device fabrication and characterisation

FTO glass was etched with zinc powder and HCl (2M) and cleaned afterwards. A compact layer of TiO_2 was deposited by spincoating a titanium isopropyl solution and heated to 500 °C for 45 minutes. After cooling down, the substrate was transferred to a nitrogen filled glovebox. A solution consisting of PbI_2 (1.25 M) and methylammoniumiodide (1.25 M) in DMF was spincoated dynamically (at 5000 rpm, total 15 sec) onto the substrate. After 5 seconds 100 µL of chlorobenzene was added on top of the spinning substrate and afterwards the substrates were placed on a hotplate (100 °C for 10 minutes). After cooling to room temperature, the hole transporter was spincoated on top. EDOT-OMeTPA (10 mg mL^{-1}), H101 (75 mg mL^{-1}) and Spiro-OMeTAD (75 mg mL^{-1}) were dissolved in chlorobenzene. *Tert*-butylpyridine (TBP; 10 µL mL^{-1}) and lithium bis(trisfluoromethylsulfonyl)imide (Li-TFSI; 30 µL mL^{-1} of a 173 mg mL^{-1} acetonitrile solution) were added to the HTM solutions. Co-dopant tris(2-(1*H*-pyrazol-1-yl)pyridine)cobalt(II)bis(hexafluorophosphate) (FK102) was predissolved in acetonitrile (150 mg mL^{-1}) and added to the HTM solution at a concentration of 0-15 mol% relative to the HTM. The thickness of the hole transport layer was found to be ~40 nm for EDOT-OMeTPA and ~250 nm for Spiro-OMeTAD and H101. The devices were stored at a relative humidity of ~30% at room temperature for 72 hours to allow the hole transporter to oxidize. The top electrode was deposited by thermal evaporation of gold under vacuum (at 10^{-6} mbar), with a thickness of 40 nm. *J-V* curves were recorded with a Keithley 2400 source meter under simulated AM 1.5G sunlight, calibrated to 100 mW cm^{-2}. The reported device characteristics were estimated from the measured *J-V* curves. The active area of the solar cells was defined with a square metal aperture mask of 0.0831 cm^2.

Microscopy

Atomic force microscopy (AFM) measurements were performed in tapping mode using a Nanoink DPN Stage microscope and scanning electron microscopy (SEM) images were obtained using a Jeol JSM-6500F microscope.

The layer thickness of Spiro-OMeTAD and the perovskite were studied by a scanning electron microscopy (SEM) cross section. The layer thickness of the hole transporter was also examined with atomic force microscopy (AFM) by spincoating a layer on glass, using the same procedure as was used for preparing the photovoltaic devices. The layer thickness of Spiro-OMeTAD measured by AFM is comparable to what was found by SEM. The H101 layer has a thickness of ~200 nm and for EDOT-OMeTPA a thickness of 35-45 nm was measured.

Synthesis and characterization

2,3-Dihydrothieno[3,4-b][1,4]dioxine-5,7-dicarboxaldehyde was crystallized twice from ethanol.

4,4'-dimethoxy-4''-nitrotriphenylamine[2]

In a dropping funnel under nitrogen, 4-nitroaniline (5.0 g, 36.2 mmol) and 1-methoxy-4-iodobezene (33 g, 140 mmol) were dissolved in DMF (150 mL). The solution was then added dropwise to a mixture of copper iodide (1.7 g, 9 mmol), potassium carbonate (38 g, 280 mmol) and L-Proline (3.3 g, 29 mmol) in a round-bottom flask under nitrogen and the reaction mixture was stirred vigorously at 115 °C. The reaction was followed by TLC and quenched after 5 days. The mixture was poured into ice water and the organics were extracted with ethyl acetate. The solution was passed through a short pad of silica gel to remove all copper salts. The resulting organic phase was concentrated under reduced pressure. After column chromatography (silica, hexanes:diethyl ether (3:1)) the product was crystalized from acetic acid and diethyl ether:hexanes to afforded the title compound as bright orange crystals (5.2 g, 41%). m.p.: 135 °C (lit.: 129–131 °C)[3,4]; ^{1}H-NMR ($CDCl_3$, 400MHz) δ: 7.97 (d, *J* = 9.3 Hz, 2H); 7.13 (d, *J* = 8.9 Hz, 4H); 6.90 (d, *J* = 8.9 Hz, 4H); 6.75 (d, *J* = 9.3 Hz, 2H); 3.81 (s, 6H) ppm; ^{13}C-NMR ($CDCl_3$, 100MHz) δ: 157.6; 154.1; 138.9; 138.2; 128.0; 125.4; 115.6; 115.1; 55.4 ppm; FTIR: 3041, 2841, 1583, 1493, 1236, 1105, 830, 748, 691 cm^{-1}; GCMS *m/z* (relative intensity): t_R = 20.6 min, 450.0 (100), 335.0 (58), 289.0 (25), 351.0 (21), 336.0 (12), 77.1 (12)

4-amino-4',4''-dimethoxytriphenylamine[2]

4,4'-dimethoxy-4''-nitrotriphenylamine (1.5 g, 4.3 mmol) was dissolved in THF (30 mL) and palladium on carbon (10%, 0.2 g) in THF (1 mL) was added to the reaction mixture. After degassing with argon for 15 minutes, the mixture was shaken under a 2.4 bar hydrogen atmosphere, using a parr hydrogenator. After 16 h the reaction mixture was filtered over a filter paper and a 0.45 µm PTFE membrane filter under nitrogen atmosphere. The solvent was removed under reduced pressure resulting in the title compound as a slightly grey solid (0.95 g; 70%). Because of the electron donating side groups this compound is very sensitive to oxygen and for that reason directly used in the next step. The material turned dark grey/black in the NMR tube in the presence of oxygen. m.p.: 135 °C (lit.: 133–134 °C)[3]; ^{1}H-NMR ($CDCl_3$, 400MHz) δ: 6.98 (d, *J* = 8.9 Hz, 4H); 6.90 (d, *J* = 8.6 Hz, 2H); 6.79 (d, *J* = 9.0 Hz; 4H); 6.59 (d, *J* = 8.7 Hz, 2H); 3.78 (s, 6H); 3.58 (s, broad, 2H) ppm; ^{13}C-NMR ($CDCl_3$, 100MHz) δ: 154.4; 142.1; 414.6; 139.9; 125.5; 124.1; 115.9; 114.3; 55.3 ppm; FTIR: 3457, 3373, 3033, 2836, 1634, 1497, 1232, 1027, 817 cm^{-1}; MS *m/z* (relative intensity): 320.0 (100), 305.0 (63), 321.1 (20), 160.0 (18), 306.0 (13)

EDOT-OMeTPA

EDOT-OMeTPA was obtained by a similar procedure as described by Petrus *et al.*[5] 4-amino-4',4''-dimethoxytriphenylamine (1.0 g, 3.1 mmol) and 2,3-dihydrothieno[3,4-b][1,4]dioxine-5,7-dicarboxaldehyde (0.26 g, 1.3 mmol) were placed in a dry round-bottom flask with condenser under a dry argon atmosphere. Dry chloroform (40 mL) was added, followed by a crystal of *p*-toluenesulfonic acid as a catalyst. The mixture turned red and was heated to reflux. After 3 days the mixture was cooled to room temperature and precipitated by adding a mixture of 2-propanol and hexane (1:4, 250 mL). The product

was filtered off and washed with 2-propanol and 2-propanol:triethylamine (98:2), resulting in a red solid. The small-molecule was dried in a vacuum oven at 60 °C (0.78 g, 0.97 mmol, 75%). m.p.: 241 °C (by DSC); ^{1}H-NMR (C_6C_6, 400MHz) δ: 8.93 (s, 2H); 7.35 (d, *J* = 8Hz, 4H) 7.28–7.15 (m); 6.84 (d, *J* = 8Hz, 8H); 3.48 (s, 4H); 3.43 (s, 12H) ppm. ^{1}H-NMR (CDCl3, 100MHz) δ: 8.60 (s, 2H); 7.13 (d, *J* = 8.8 Hz, 4H); 7.05 (d, *J* = 2.4 Hz, H); 6.92 (d, *J* = 8.8 Hz, 4H); 6.82 (d, *J* = 8.8 Hz, 8H); 4.35 (s, 4H); 3.80 (s, 12H) ppm; ^{13}C-NMR ($CDCl_3$, 100MHz) δ: 155.7; 147.3; 145.9; 143.9; 143.2; 140.9; 126.3; 122.2; 121.2; 121.0; 114.6; 65.0; 55.5 ppm; FTIR: 3039, 2928, 2833, 1603, 1496, 1236, 1082, 1034, 823, 721, 577 cm^{-1};

Thermal properties of the small-molecule

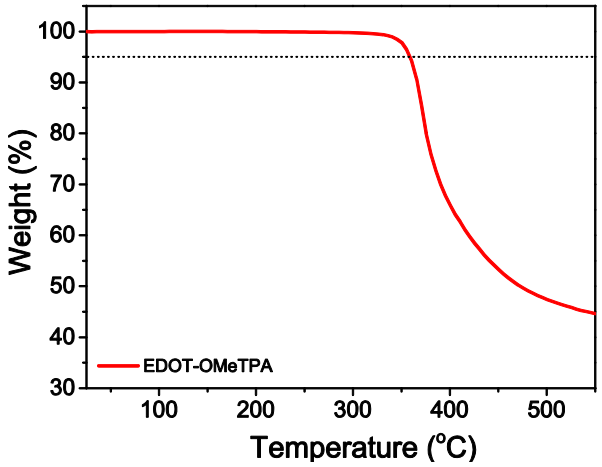

Figure S1: TGA thermograms of the azomethine-based small-molecule at a heating rate of 10 °C min^{-1} under nitrogen after drying at 220 °C.

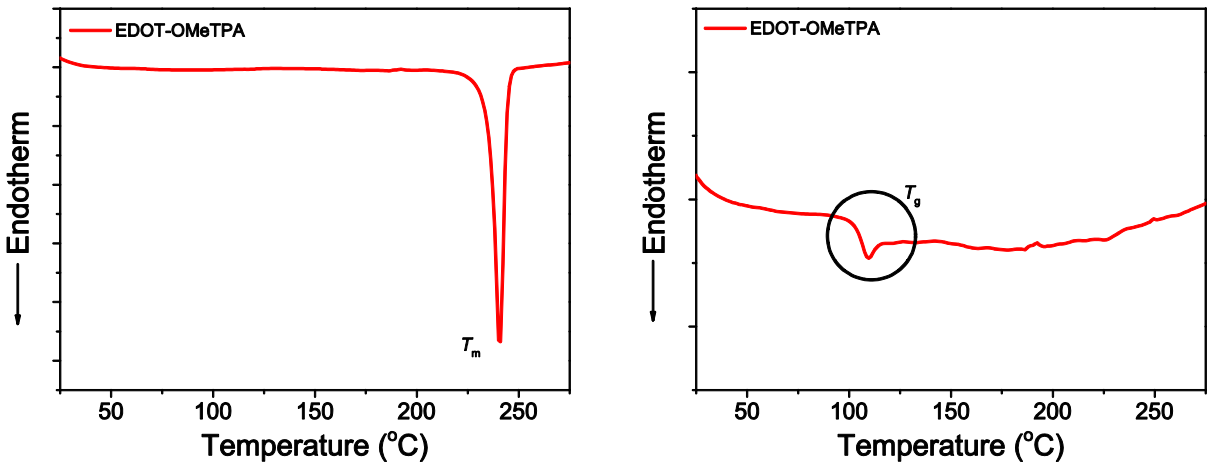

Figure S2: DSC curves of the azomethine based small-moleule at a heating rate of 20 °C min^{-1} under nitrogen. Left, first heating showing the melting endotherm, which is only observed in the first cycle. Right, second heating clearly showing the glass transition temperature (T_g) just above 100 °C.

Optoelectronic properties

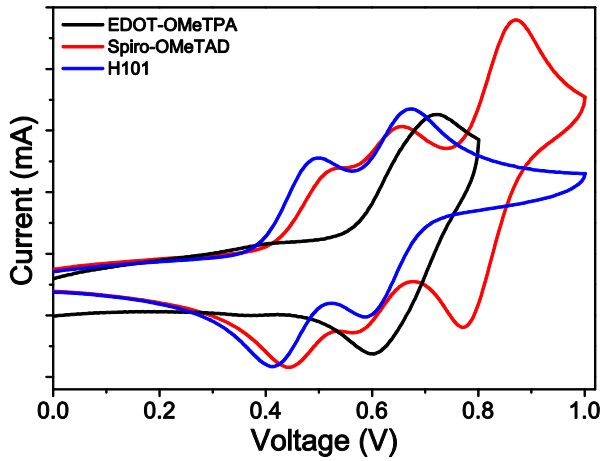

Figure S3: Cyclic voltammograms of EDOT-OMeTPA, Spiro-OMeTAD and H101 measured in a dichloromethane solution containing $tBuNPF_6$ as electrolyte.

Table S1: Optoelectronic properties of EDOT-OMeTPA and the reference materials Spiro-OMeTAD and H101.

HTM[a]	HOMO (eV)	LUMO[a] (eV)	λ_{max} (nm)	λ_{onset} (nm)	E_g (eV)	T_g (°C)	T_m (°C)	$T_d^{5\%}$ (°C)
EDOT-OMeTPA	-5.28	-3.3	505	625	2.0	105	241	359
Spiro-OMeTAD	-5.13	-2.1	377	420	3.0	125[c]	248[c]	-
H101	-5.09	-2.4	405	460	2.7	73[b]	-	-

[a] estimated by adding the optical bandgap to the HOMO energy level, [b] published by Li *et al.*[6], [c] published by Leijtens *et al.*[7]

T_g = glass transition temperature, T_m = melting temperature

Photovoltaic properties

Cobalt dopant

The work by Li *et al.*[6] showed a significant improvement in the power conversion efficiency by adding cobalt dopent FK102 to the hole transporter H101. Similar to their work we added 5; 10 and 15 mol% FK102 to our azomethine based hole transporter. However, no improvement in the device performance was observed.

Azomethine vs no HTM

Since the layer thickness of the azomethine hole transporter is relatively thin, we also prepared devices without any transport layer to see the effect of the azomethine. We spincoated chlorobenzene and chlorobenzene with the standard additive (LiTFSI and *t*BP) on top of the perovskite before depositing the gold electrode.

All devices without a hole transport layer, using only gold as a "selective" electrode, showed poor efficiencies and most devices were shorted. When only chlorobenzene was used the best efficiency obtained was 0.3%. When the dopants were added to the chlorobenzene efficiencies up to 3.7% were reached. This shows that, although the azomethine hole transport layer is thin, it does improve the device performance significantly and also reduces the amount of shorted devices.

Average of devices

Here we present the averages of the devices characteristics measured. While the currents and fill factors are rather comparable for the three different hole transporting materials, the difference arises from the open circuit voltage. As a result of the small loss in V_{oc} for the EDOT-OMeTPA devices compared to Spiro-OMeTAD the PCE is slightly lower. However, the V_{oc} is generally easily optimized by aligning the energy levels. The good currents and fill factor show that azomethines are a promising hole transporting material.

We also observed that devices with the azomethine as hole transport material were considered shorted more often compared to Spiro-OMeTAD. This might be the result of the relatively thin azomethine hole transport layer, which could also explain the relatively large standard deviation for the efficiency. However, also H101 showed significant more shorted devices compared to Spiro-OMeTAD.

When a concentration of 10 mg mL^{-1} was used for spincoating Spiro-OMeTAD as HTM, most of the devices were considered shorted (16 out of the 24) and the efficiencies of the "working" devices were significantly lower (average PCE = 4.8%). This shows that lowering the concentration and the layer thickness does not always result in better performance.

Table S2: Average J-V characteristics of the photovoltaic devices with different HTMs.

HTM[a]	J_{sc} (mA cm^{-2})	V_{oc} (V)	**FF** (%)	**PCE** (%)	**Number of devices/of which showed strong shunting**
EDOT-OMeTPA	12.2 ± 2.5	0.83 ± 0.10	0.64 ± 0.13	6.6 ± 2.2	24/7
Spiro-OMeTAD	13.4 ± 3.2	0.97 ± 0.03	0.67 ± 0.08	9.2 ± 1.6	24/2
H101	13.6 ± 5.4	0.88 ± 0.04	0.49 ± 0.06	7.2 ± 1.7	24/6

[a] LiTFSI and tBP were added as dopants to the HTM layer.

Hysteresis

All devices suffer from significant hysteresis between the forward and backward scan.

Table S3: Power conversion efficiencies obtained from the J-V curves when scanned forward or backwards.

HTM[a]	$PCE_{Forwards}$ (%)	$PCE_{Backwards}$ (%)
EDOT-OMeTPA	6.2	11.0
Spiro-OMeTAD	7.1	11.9
H101	5.9	10.9

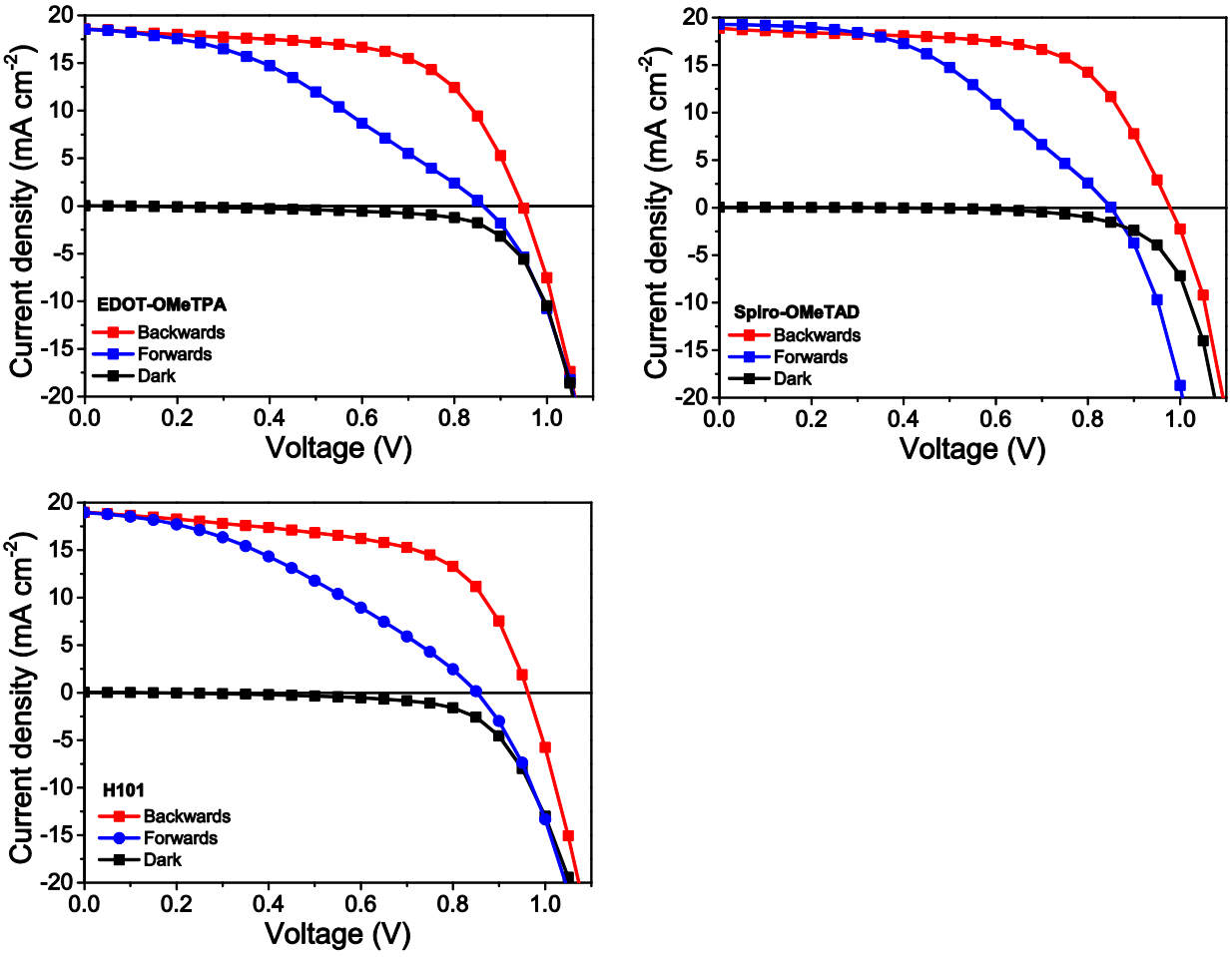

Figure S4: Forward, backward and dark scans of the "record" perovskite devices using different hole transporting materials.

Stability

Representative photovoltaic devices with Spiro-OMeTAD and EDOT-OMeTPA as hole transporting layer and without encapsulation were aged at ambient temperature in the dark at a relative humidity of around 30%. The *J-V* curves of the freshly prepared devices were recorded and compared to the *J-V* curves obtained after 1000h of ageing (Figure S5). A rather small loss of around 10% of the original PCE was observed after 1000 hours for both EDOT-OMeTPA and Spiro-OMeTAD. The main loss was found in the J_{sc}, which is in accordance with literature.[8] Additionally we observed that in the first days the PCE slightly increases, which we ascribe to oxidation of the hole transporter under the influence of oxygen. The highest efficiencies are generally measured after 3 days.

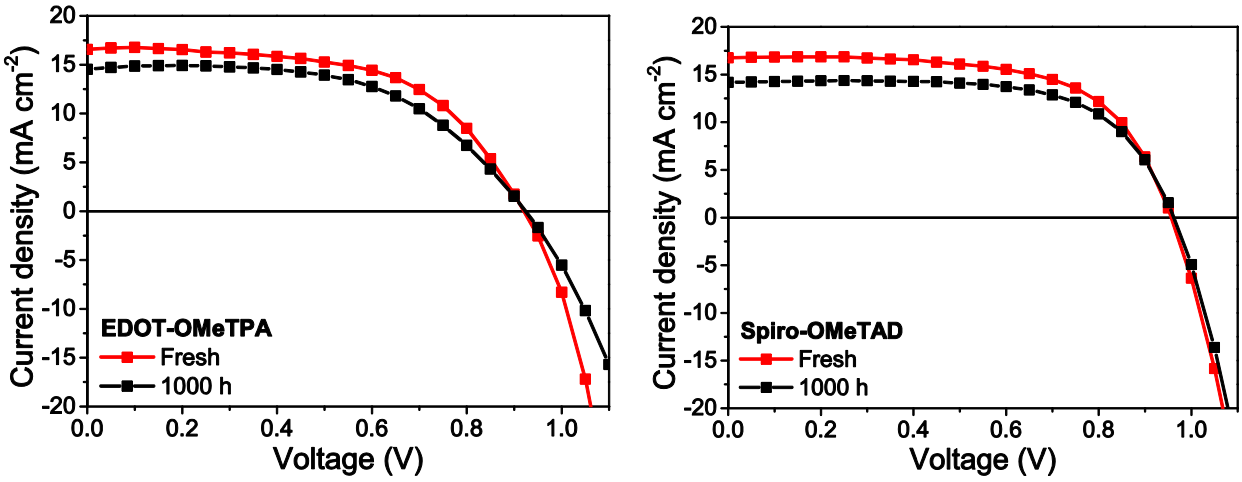

Figure S5: J-V curves of representative devices with different hole transporting materials showing the characteristics for freshly prepared devices and the performance after 1000 hours of ageing.

Cost estimation of hole transporter for 1 m^2.

We estimated the cost for the hole transporting layer for a solar cell. We like to note that this is a very rough estimation, in part as a result of the estimated cost of EDOT-OMeTPA, which is described below. Nevertheless, the estimated cost for EDOT-OMeTPA is more than two orders of magnitude lower compared to state-of-the-art materials.

State-of-the-art HTM (Spiro-OMeTAD or H101)

We assume a 200 nm thick HTM layer and no loss of hole transporting material during the processing. This results in 0.2 cm^3 of HTM per m^2. Assuming a density of 1 g cm^{-3} and a price of 200 \$ g^{-1}, this would result in a cost of \$40 per square meter of solar cell.[9] The cost is estimated from the commercial price for Spiro-OMeTAD and H101.

EDOT-OMeTPA

We assume a 40 nm thick HTM layer and no loss of hole transporting material during the processing. This results in 0.04 cm^3 of HTM per m^2. Assuming a density of 1 g cm^{-3} and a price of 9.57 \$ g^{-1}, this would result in a cost of \$0.38 per square meter of solar cell. For optimizing the device reproducibility thicker HTM layers might be required; although this would increase the cost for EDOT-OMeTPA, the significantly lower material cost will still result in a significant lower materials cost.

Cost-per-peak-Watt

In order to estimate the cost-per-peak-Watt we used the model as was established by Osedach *et al.*[10] The cost-per-peak-Watt (\$ per W_p, denoted here as C_w) was calculated using this equation:

$$C_w = \frac{C_g \times \rho \times L}{PCE \times I}$$

Here, C_g is the cost per gram, ρ is the density of the hole transporter (assumed to be 1 g cm^{-3}), L is the hole transporter layer thickness, PCE is the power conversion efficiency, I is the solar insolation under peak condition, assumed to be 1000 W m^{-2}.

This result in a cost-per-peak-Watt of 0.004 \$ W^{-1} for EDOT-OMeTPA.

On the other hand for state-of-the-art materials (assuming a 200 nm thick layer and a cost of 200 \$ g^{-1}) the cost-per-peak-Watt would be 0.34 \$ W^{-1}.

Assuming a target module cost of 0.50 \$ per W_p,[11] this would result in a contribution of less than 1% for EDOT-OMeTPA, which could be considered as negligible.[10] In contrast, the contribution of state-of-the-art materials will exceed the 50% of the targeted module cost.

Cost model

In order to make an estimate of the cost of the different hole transporting materials using the cost model as was described by Osedach *et al.*[10] For every synthetic step the required amounts of reactants, catalysts, reagents and solvents are calculated to obtain 1 gram of the final product. Additionally, the required materials for workup and purification were estimated using the procedure as published.[10]

1. Quenching/neutralization. The required amounts were evaluated on a case-by-case basis. For neutralization a stoichiometric amount of the acid or base were assumed to be necessary.

2. Extraction: The use of 150 mL solvent (three times 50 mL) and 1 gram of drying agent (Na_2SO_4, or $MgSO_4$) were assumed to be required to obtain 1 gram of the (intermediate) product.

3. Column chromatography. We assume that to obtain 1 gram of the (intermediate) product, 400 mL of solvent and a column filled with 263 g of 60 µm silica gel was used. The amounts are based on the assumption that the separation (R_f > 0.3) and sample loading would be ideal.

4. Recrystallization. We assume that 1 gram of product requires 100 mL of solvent and that the procedure is only performed once.

5. Distillation/sublimation. We assume no chemicals are required and no chemical waste, the energy was similar to other steps not included.

6. Washing. We assume 100 mL of solvent is required to wash 1 gram of the (intermediate) product.

7. Filtering. We assume 50 mL of solvent is required to filter 1 gram of the (intermediate) product.

The quantities are based on published procedures where the synthesis, workup and purification are performed on a lab scale. Upscaling to a multi-kilogram scale might reduce the quantities, especially materials used in the purification, considerably. For example, multiple steps could possibly be combined to reduce the number of isolation steps ("telescoping"). Also solvents might be replaced for cheaper (and/or environmentally friendly) alternatives or reused to reduce materials and waste cost. For this reason the estimated material cost could be seen as an upper limit.

The starting materials and therefore the amount of synthetic steps could be a topic of debate, however most of the used starting materials are common starting materials for the different synthetic routes. In example, 4-iodoaniline has been used as starting material for all three protocols.

In order to estimate the cost, quotes (for bulk quantities when possible) have been collected from major chemical suppliers (Sigma-Aldrich, Acros Organics and Fischer Chemicals) for all used chemicals. The costs were multiplied by the quantities that are required for the synthesis and the sum of all costs was calculated to estimate to total material cost.

Different synthetic routes were evaluated in order to find the most cost effective route. We found that especially procedures that require column chromatography for purification add significantly to the cost, as a result of the high prices of silica gel together with the large amounts of solvent used. Also upscaling of column chromatography to a multi-kilogram scale will be challenging.

Furthermore, production on a large scale could have an influence on the price of starting materials. The cost of starting materials might be reduced significantly. Also by finding other suppliers of chemicals the cost of (especially organic) starting materials could be further reduced. In example, 3,4-ethylenedioxythiophene (EDOT) is commercially available at Sigma-Aldrich and Acros organics in small quantities at prices exceeding $5,000 per kilogram, while other suppliers offer the same material in an even higher purity in bulk quantities at prices below $250 per kilogram.

We also note that the material cost only takes into account the cost of materials used. Equipment, energy consumption, maintenance, waste treatment, labor, profit and various other overhead charges are not taken into account. Depending on the synthesis and purification steps this could also have a significant influence on the cost. For example, palladium cross-coupling reactions require stringent conditions, making the upscaling significant more costly than simple reactions that can be performed at ambient conditions. In the case of pharmaceutical drugs, for example, the materials cost accounts for only 20-45% of the total cost of drug synthesis.

Spiro-OMeTAD

The synthesis of Spiro-OMeTAD has been well described in the literature and several synthetic routes were evaluated. Spiro-biflourene is an expensive starting material because the synthesis of this material requires several synthetic steps. The final palladium catalyzed reaction requires column chromatography as purification step.

H101

Unfortunately only few synthetic routes towards H101 have been reported in literature. The limited synthetic details used in the work of Lambert *et al.*[12] and Lin *et al.*[13] limits us to use the synthetic route of Teng *et al.*[14] to obtain the triphenylamine-based boronic acid. Although only 3 synthetic steps are required, the estimated materials cost is higher than for Spiro-OMeTAD. This could be ascribed to the purification of the intermediates that all require column chromatography according to literature procedures. As described before, telescoping is expected to reduce the purification steps and therefore the cost of H101 could possibly be reduced.

EDOT-OMeTPA

The synthesis op EDOT-OMeTPA requires 4 synthetic steps. However, the synthetic protocols are generally simple and the (intermediate) products can be purified easily. For example no column chromatography is required to purify the products, as water is the only byproduct in the final condensation reaction. This results in a low material cost, which is about an order of magnitude lower compared to H101 and Spiro-OMeTAD. Also the fact that the condensation reaction can be performed at near ambient conditions simplifies the synthesis and therefore the equipment required to produce these materials on a large scale.

Commercial prices

We compare the estimated materials cost with the commercial prices of Spiro-OMeTAD and H101. Similar to the estimated materials cost, the commercial prices of H101 and Spiro-OMeTAD are rather comparable. The commercial price is a bit more than twice as high as the estimated material cost, which could be explained by the additional costs as was described before.

Table S4: Survey of the estimated materials cost for the synthesis of different hole transporting materials.

HTM	**Steps**	**Waste** (kg/g)	**Halogen rich solvents** (kg/g)	**Reagents** ($/g)	**Solvent** ($/g)	**Workup** ($/g)	**Cost** ($/g)	**Commercial price** ($/g)
EDOT-OMeTPA	4	0.7	0.1	5.73	1.42	2	9.57	n/a
Spiro-OMeTAD	6	3.6	1.0	6.14	2.06	83	91.67	170-475
H101	3	4.0	2.3	7.64	0.46	103	110.96	250

Waste and environmental impact

From Table S4 it is clear that the synthesis of H101 and Spiro-OMeTAD also results in significantly more waste. The total amount of chemicals required is more than 5 times more for Spiro-OMeTAD and H101 compared to EDOT-OMeTPA. Besides the cost for buying the chemicals and the waste treatment, many chemicals also have a significant impact on the environment. Especially halogenated solvents are known to cause a serious health risk and are often carcinogenic to humans. The synthesis of Spiro-OMeTAD and H101 require 1.0 kg and 2.3 kg of halogenated solvents respectively, in contrast, the synthesis of EDOT-OMeTPA requires only 0.1 kg of halogenated solvents per gram of product.

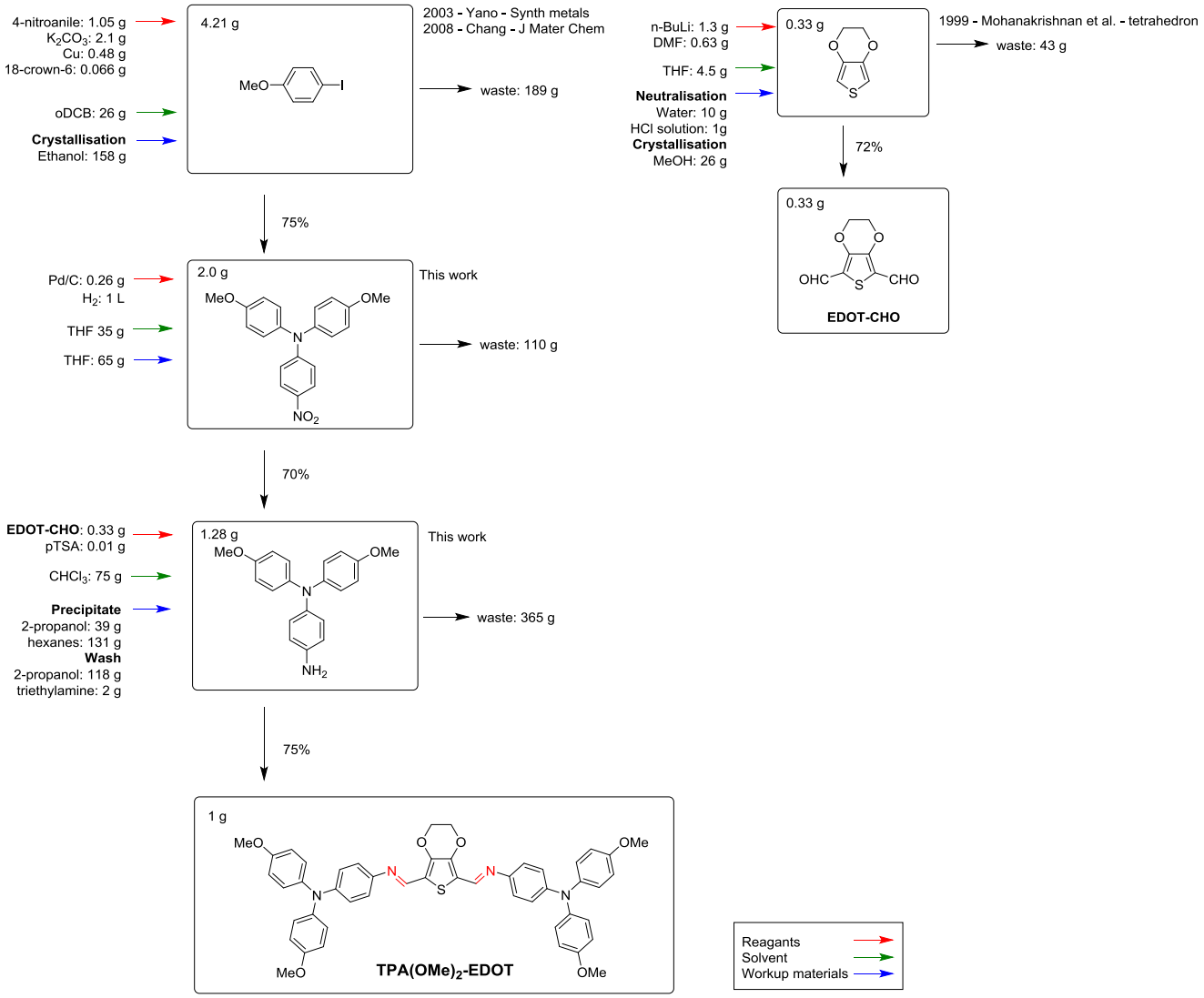

Figure S6: Flowchart describing the synthesis of 1 gram of EDOT-OMeTPA route 1.[15–17]

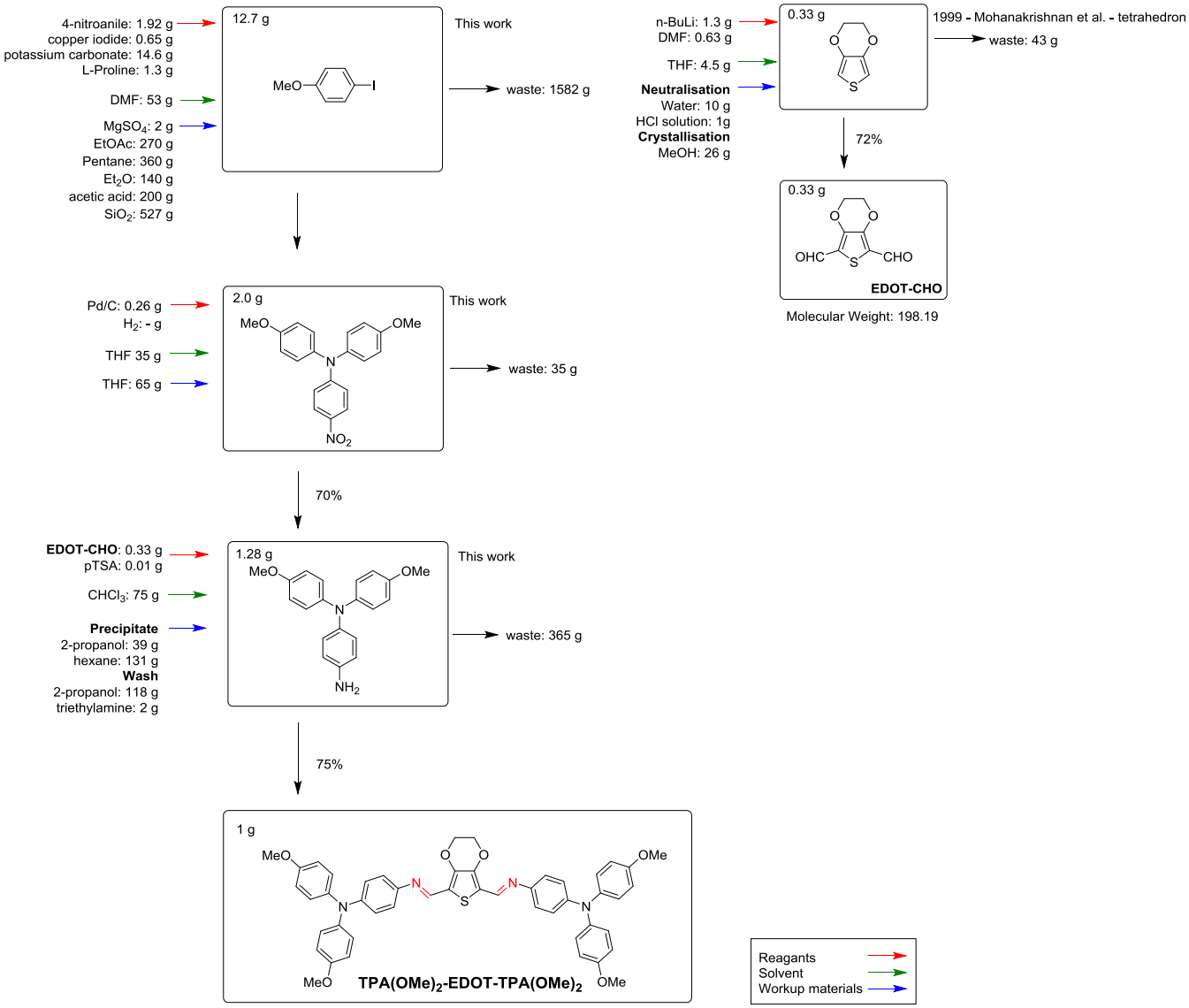

Figure S7: Flowchart describing the synthesis of 1 gram of EDOT-OMeTPA route 2.[17]

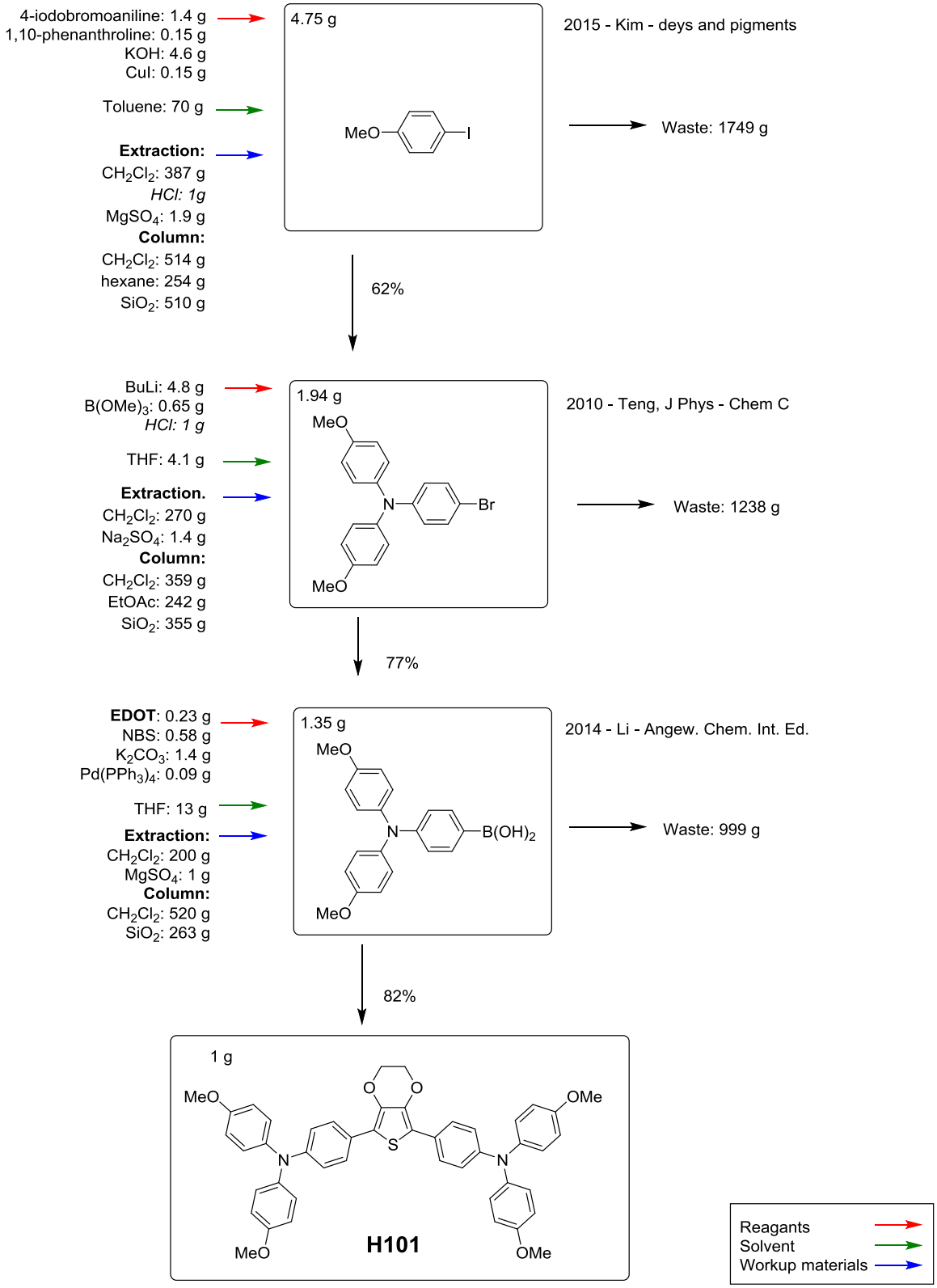

Figure S8: Flowchart describing the synthesis of 1 gram of H101 route 1.[6,14,18]

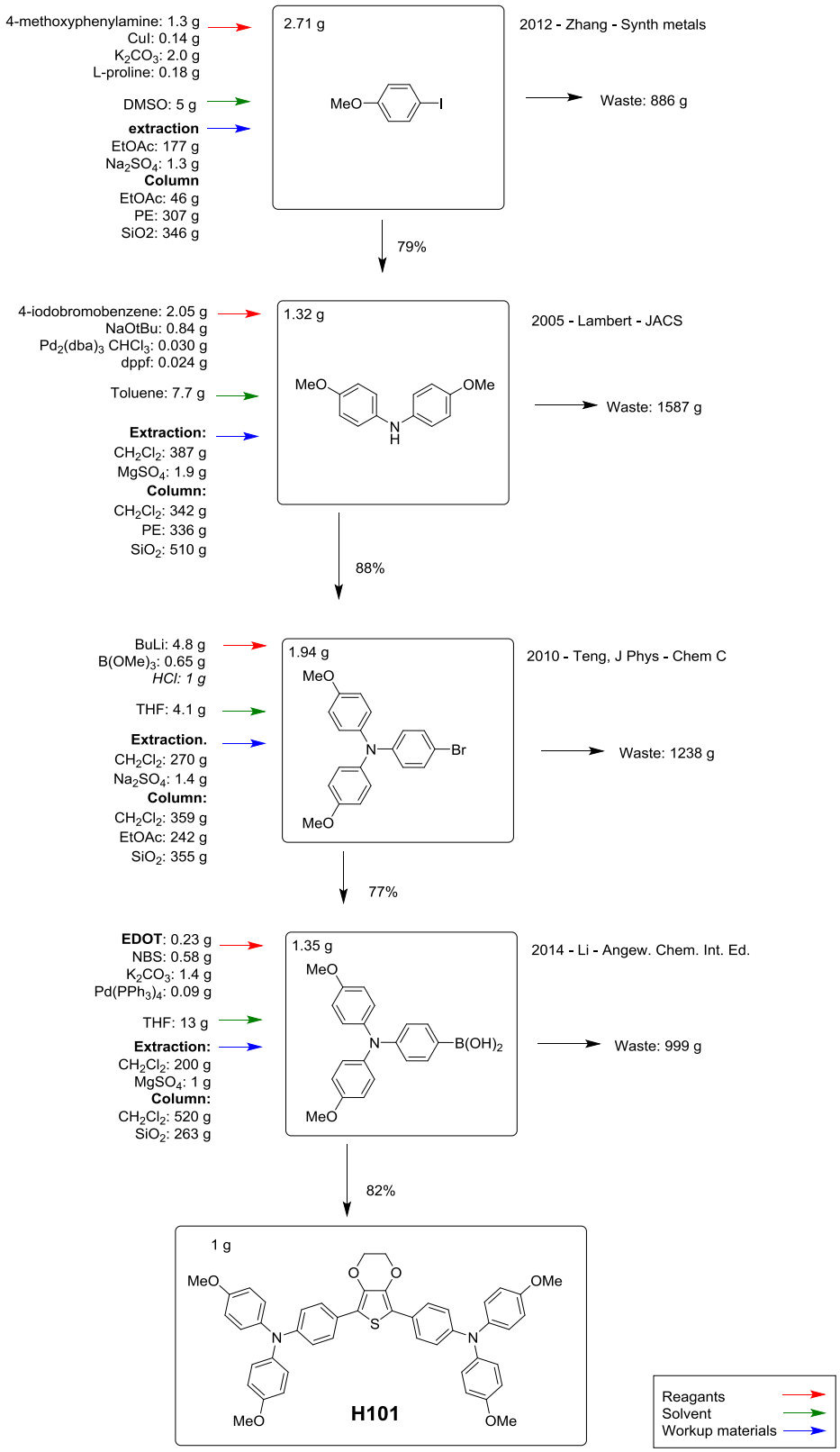

Figure S9: Flowchart describing the synthesis of 1 gram of H101 route 2.[6,14,19,20]

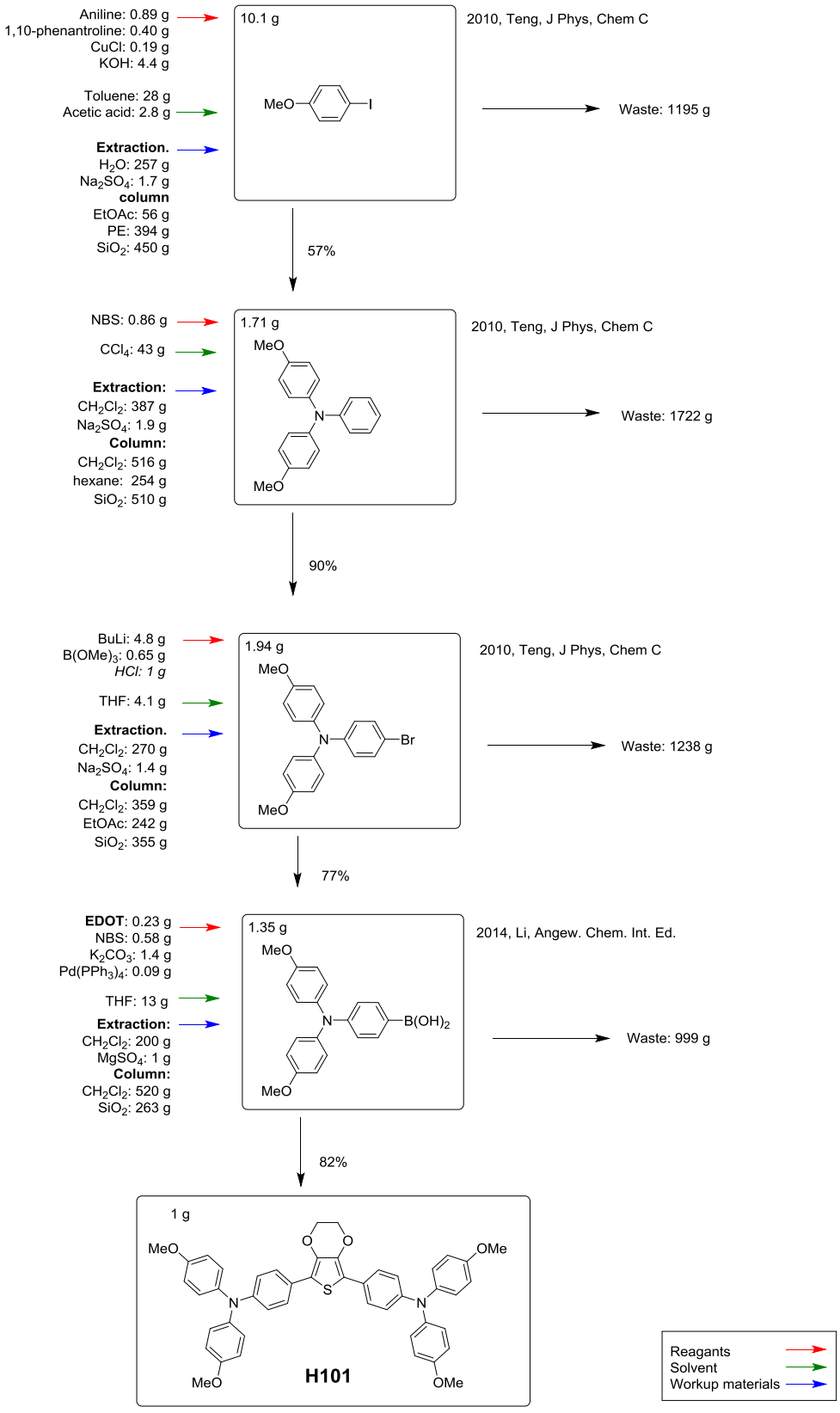

Figure S10: Flowchart describing the synthesis of 1 gram of H101 route 3.[6,14]

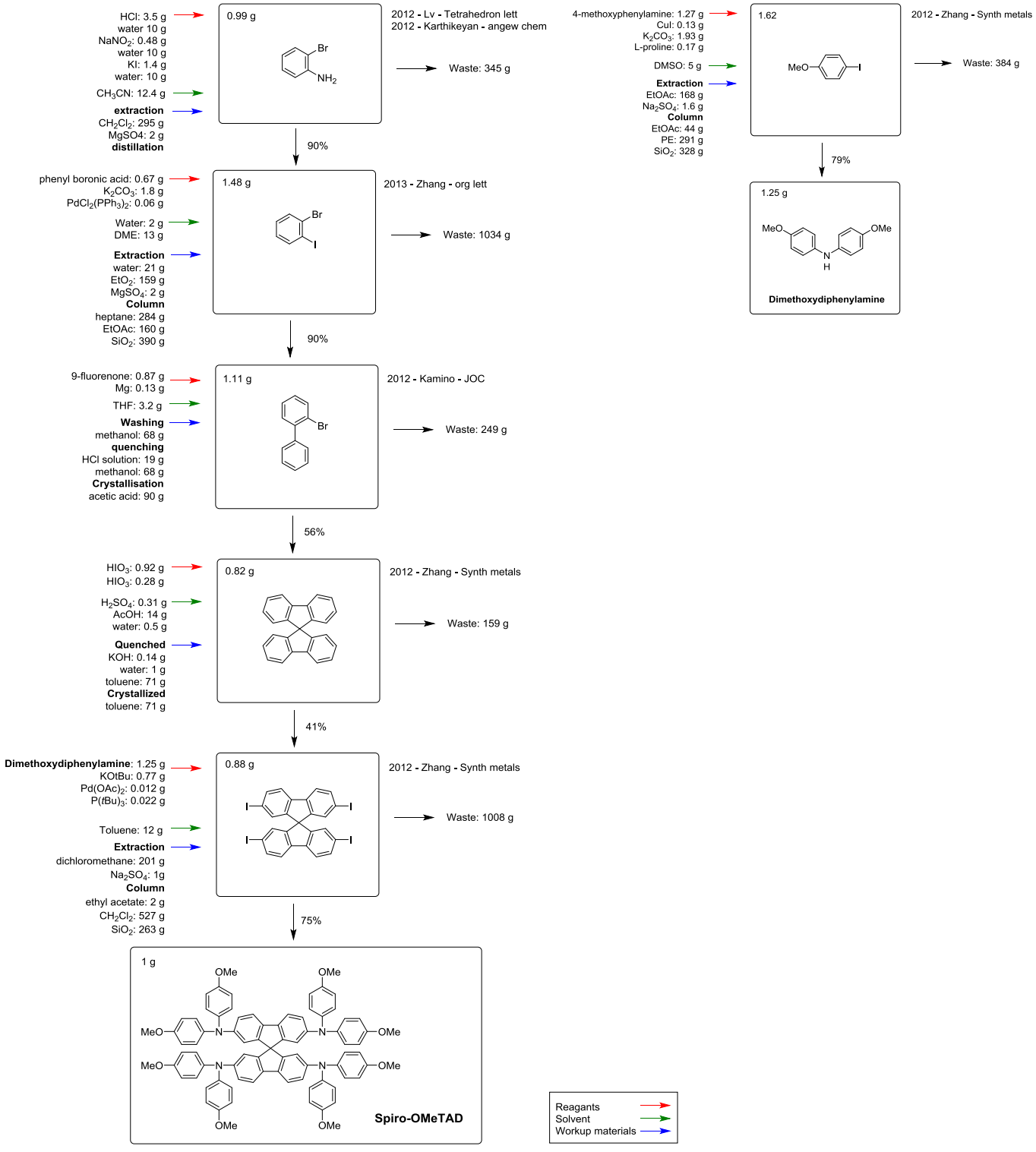

Figure S11: Flowchart describing the synthesis of 1 gram of Spiro-OMeTAD route 1.[21–25]

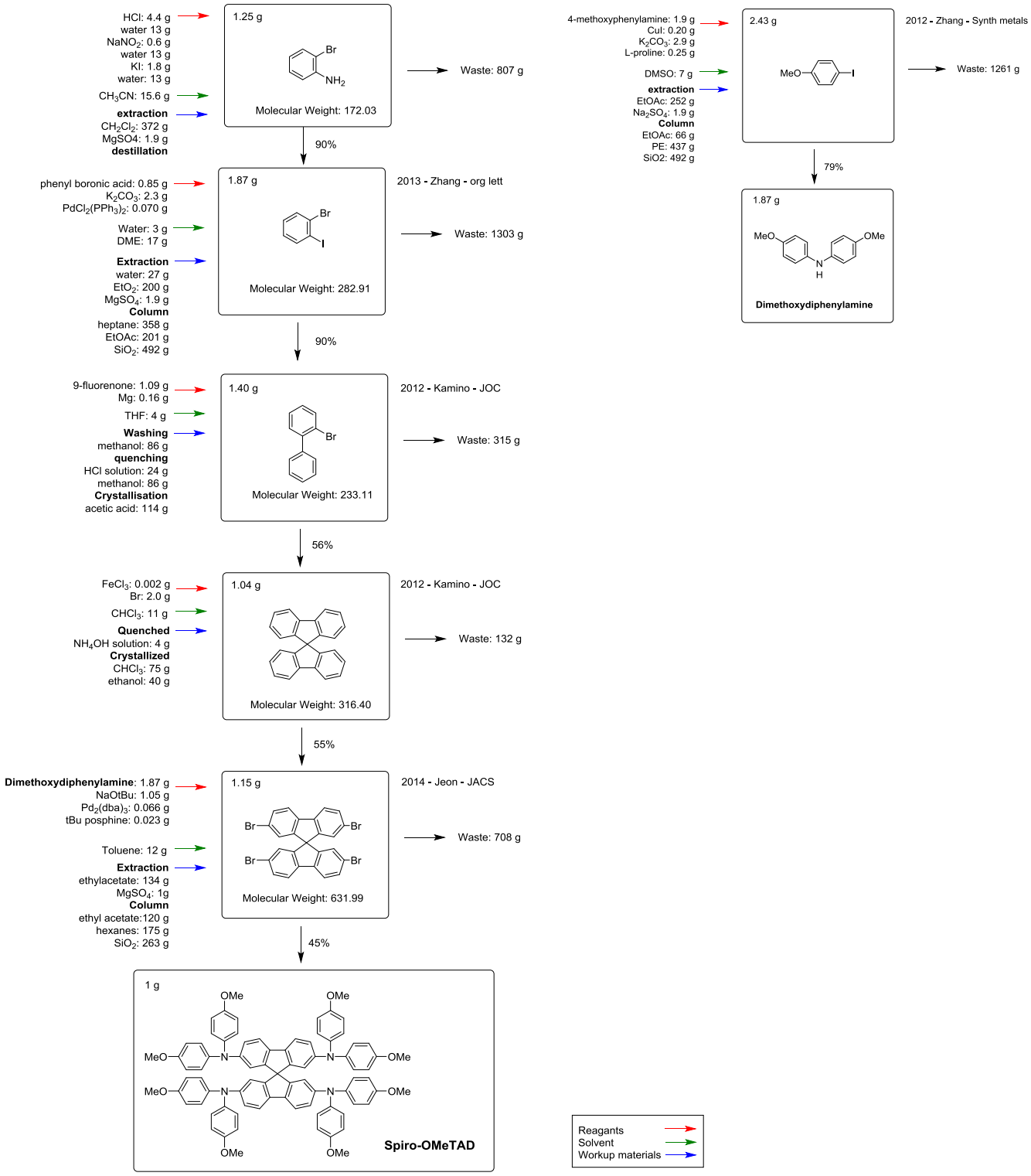

Figure S12: Flowchart describing the synthesis of 1 gram of Spiro-OMeTAD route 2.[21–26]

Table S5: Materials quantities and cost for the synthesis of EDOT-OMeTPA via route 1.

Chemical name	Weight reagent (g/g)	Weight solvent (g/g)	Weight workup (g/g)	Price of Chemical ($/kg)	Material cost ($/g product)	Cost per step ($/step)
EDOT	0.33			4,9442.88	1.63	1.92
n-Butyl lithium (2.5 M)	1.3			96.05	0.12	
Dimethylformamide	0.63			5.09	0.00	
Tetrahydrofuran		4.5		9.94	0.04	
Hydrochloric acid			1	62.60	0.06	
Water			10	0.00	-	
Methanol			26	2.21	0.06	
4-Nitroanline	1.05			239.56	0.25	3.45
4-Iodoanisole	4.21			510.31	2.15	
K_2CO_3	2.1			6.74	0.01	
Copper powder	0.48			66.26	0.03	
18-crown-6	0.066			2,511.09	0.17	
o-dichlorobenzene		26		11.26	0.29	
Ethanol			158	3.48	0.55	
Hydrogen*	*1**			*5.13**	0.01	2.36
Pd/C (10%)	0.26			5,155.06	1.34	
Tetrahydrofuran		35		9.94	0.36	
Tetrahydrofuran			65	9.94	0.65	
p-toluenesulfonic acid	0.01			23.39	0.00	1.84
Chloroform		75		2.60	0.20	
Hexane		131		6.79	0.89	
Isopropanol		39		4.50	0.18	
Isopropanol			118	4.50	0.53	
Triethylamine			2	23.18	0.05	
Total	**14.7**	**310**	**380**	**-**	**-**	**9.57**

* as gas in liters ($/L)

Table S6: Materials quantities and cost for the synthesis of EDOT-OMeTPA via route 2.

Chemical name	**Weight reagent (g/g)**	**Weight solvent (g/g)**	**Weight workup (g/g)**	**Price of Chemical ($/kg)**	**Material cost ($/g product)**	**Cost per step ($/step)**
EDOT	0.33			4,9442.88	1.63	1.92
n-Butyl lithium 2.5M	1.3			96.05	0.12	
Dimethylformamide	0.63			5.09	0.00	
Tetrahydrofuran		4.5		9.94	0.04	
Hydrochloric acid			1	62.60	0.06	
Water			10	0.00	-	
Methanol			26	2.21	0.06	
4-Nitroaniline	1.92			239.56	0.56	57.26
4-Iodoanisole	12.7			510.31	6.48	
Copper(I) iodide	0.65			115.74	0.08	
K_2CO_3	14.6			6.74	0.10	
L-Proline	1.3			90.63	0.12	
Dimethylformamide		53		5.09	0.27	
$MgSO_4$			2	54.24	0.11	
Ethyl acetate			270	3.63	0.98	
Hexanes			360	6.79	2.44	
Diethyl ether			140	22.89	3.20	
Acetic acid			200	40.12	8.02	
Silica gel			527	66.41	35.00	
Hydrogen*	*1**			*5.13**	0.01	2.36
Pd/C (10%)	0.26			5,155.06	1.34	
Tetrahydrofuran		35		9.94	0.36	
Tetrahydrofuran			65	9.94	0.65	
p-toluenesulfonic acid	0.01			23.39	0.00	1.84
Chloroform		75		2.60	0.20	
Hexanes		131		6.79	0.89	
Isopropanol		39		4.50	0.18	
Isopropanol			118	4.50	0.53	
Triethylamine			2	23.18	0.05	
Total	**38**	**337**	**1721**	**-**	**-**	**63.39**

* as gas in liters ($/L)

Table S7: Materials quantities and cost for the synthesis of H101 via route 1.

Chemical name	Weight reagent (g/g)	Weight solvent (g/g)	Weight workup (g/g)	Price of Chemical ($/kg)	Material cost ($/g product)	Cost per step ($/step)
4-Iodoanisole	4.75			510.31	2.42	50.07
4-Bromoaniline	1.4			545.79	0.76	
1,10-Phenantroline	0.15			4,423.95	0.66	
Potassium hydroxide	4.6			21.21	0.10	
Copper(I) iodide	0.15			115.74	0.02	
Toluene		70		4.08	0.29	
Dichloromethane			387	11.16	4.32	
Hydrochloric acid			1	62.60	0.06	
$MgSO_4$			1.9	54.24	0.10	
Dichloromethane			514	11.16	5.74	
Hexanes			254	6.79	1.72	
Silica gel			510	66.41	33.87	
n-Butyl lithium (1.6 M)	4.8			144.94	0.70	32.36
Trimethyl borate	0.65			104.57	0.07	
Hydrochloric acid	1			63.60	0.06	
Tetrahydrofuran		4.1		9.94	0.04	
Dichloromethane			270	11.16	3.01	
Na_2SO_4			1.4	12.79	0.02	
Dichloromethane			359	11.16	4.01	
Ethyl acetate			242	3.63	0.88	
Silica gel			355	66.41	23.58	
EDOT	0.23			4,9442.88	1.14	28.53
N-Bromosuccinimide	0.58			82.20	0.05	
K_2CO_3	1.4			6.74	0.01	
$Pd(PPh_3)_4$	0.09			18,364.76	1.65	
Tetrahydrofuran		13		9.94	0.13	
Dichloromethane			200	11.16	2.23	
$MgSO_4$			1	54.25	0.05	
Dichloromethane			520	11.16	5.80	
Silica gel			263	66.41	17.47	
Total	**19.8**	**87.1**	**3986**	**-**	**-**	**110.96**

Table S8: Materials quantities and cost for the synthesis of H101 via route 2.

Chemical name	Weight reagent (g/g)	Weight solvent (g/g)	Weight workup (g/g)	Price of Chemical ($/kg)	Material cost ($/g product)	Cost per step ($/step)
1-Iodoanisole	2.71			510.31	1.38	29.73
4-Methoxyphenylamine	1.3			128.82	0.17	
Copper(I) iodide	0.14			115.74	0.02	
K_2CO_3	2			6.74	0.01	
L-proline	0.18			90.63	0.02	
Dimethyl sulfoxide		5		8.52	0.04	
Ethyl acetate			177	3.63	0.64	
Na_2SO_4			1.3	12.79	0.02	
Ethyl acetate			46	3.63	0.17	
Petroleum ether			307	13.95	4.28	
Silica gel			346	66.41	22.98	
4-Bromobenzene	2.05			5,491.80	11.26	61.09
Sodium *t*-butoxide	0.84			227.30	0.19	
$Pd_2(dba)_3$ $CHCl_3$	0.030			76,342.00	2.29	
dppf*	0.024			22,012.00	0.53	
Toluene		7.7		4.08	0.03	
Dichloromethane			387	11.16	4.32	
$MgSO_4$			1.9	54.24	0.10	
Dichloromethane			342	11.16	3.82	
Petroleum ether			336	13.95	4.69	
Silica gel			510	66.41	33.87	
n-Butyl lithium (1.6 M)	4.8			144.94	0.70	32.36
Trimethyl borate	0.65			104.57	0.07	
Hydrochloric acid	1			63.60	0.06	
Tetrahydrofuran		4.1		9.94	0.04	
Dichloromethane			270	11.16	3.01	
Na_2SO_4			1.4	12.79	0.02	
Dichloromethane			359	11.16	4.01	
Ethyl acetate			242	3.63	0.88	
Silica gel			355	66.41	23.58	
EDOT	0.23			4,9442.88	1.14	28.54
N-Bromosuccinimide	0.58			82.20	0.05	
K_2CO_3	1.4			6.74	0.01	
$Pd(PPh_3)_4$	0.09			18,364.76	1.65	
Tetrahydrofuran		13		9.94	0.14	
Dichloromethane			200	11.16	2.23	
$MgSO_4$			1	54.25	0.05	
Dichloromethane			520	11.16	5.80	
Silica gel			263	66.41	17.47	
Total	**18.0**	**29.8**	**4714**	**-**	**-**	**151.72**

* 1,1'-Bis(diphenylphosphino)ferrocene

Chemical name	Weight reagent (g/g)	Weight solvent (g/g)	Weight workup (g/g)	Price of Chemical ($/kg)	Material cost ($/g product)	Cost per step ($/step)
4-Iodoanisole	10.12			510.31	5.16	42.96
Aniline	0.89			96.05	0.09	
1,10-phenantroline	0.4			4423.95	1.77	
Copper(I) chloride	0.19			69.74	0.01	
Potassium hydroxide	4.4			21.21	0.09	
Toluene		28		4.08	0.11	
Acetic acid		2.8		40.12	0.11	
Water			257	0.00	0.00	
Na_2SO_4			1.7	12.79	0.02	
Ethyl acetate			56	3.63	0.20	
Petroleum ether			394	13.95	5.50	
Silica gel			450	66.41	29.88	
N-Bromosuccinimide	0.86			82.20	0.07	50.96
CCl_4		43		120.87	5.20	
Dichloromethane			387	11.16	4.32	
Na_2SO_4			1.9	12.79	0.02	
Dichloromethane			516	11.16	5.76	
Hexane			254	6.79	1.72	
Silica gel			510	66.41	33.87	
Butyl lithium (1.6M)	4.8			144.94	0.70	32.36
Trimethylborate	0.65			104.57	0.07	
Hydrochloric acid	1			63.60	0.06	
tetrahydrofuran		4.1		9.94	0.04	
dichloromethane			270	11.16	3.01	
Na_2SO_4			1.4	12.79	0.02	
Dichloromethane			359	11.16	4.01	
Ethyl acetate			242	3.63	0.88	
Silica gel			355	66.41	23.58	
EDOT	0.23			4,9442.88	1.14	28.54
N-Bromosuccinimide	0.58			82.20	0.05	
K_2CO_3	1.4			6.74	0.01	
$Pd(PPh_3)_4$	0.09			18,364.76	1.65	
Tetrahydrofuran		13		9.94	0.14	
Dichloromethane			200	11.16	2.23	
$MgSO_4$			1	54.25	0.05	
Dichloromethane			520	11.16	5.80	
Silica gel			263	66.41	17.47	
Total	**25.6**	**90.9**	**5039**	**-**	**-**	**154.81**

Table S9: Materials quantities and cost for the synthesis of Spiro-OMeTAD via route 1.

Chemical name	Weight reagent (g/g)	Weight solvent (g/g)	Weight workup (g/g)	Price of Chemical ($/kg)	Material cost ($/g product)	Cost per step ($/step)
1-Iodoanisole	1.62			510.31	0.83	27.71
4-Methoxyphenylamine	1.27			128.82	0.16	
Copper(I) iodide	0.13			115.74	0.02	
K_2CO_3	1.93			6.74	0.01	
L-Proline	0.17			90.63	0.02	
Dimethyl sulfoxide		4.67		8.52	0.04	
Ethyl acetate			168	3.63	0.61	
Na_2SO_4			1	12.79	0.02	
Ethyl acetate			44	3.63	0.16	
Petroleum ether			291	13.95	4.06	
Silica gel			328	66.41	21.78	
2-Bromoanline	0.99			706.70	0.70	4.54
Hydrochloric acid	3.49			62.60	0.22	
Water	10.32			-	-	
$NaNO_2$	0.48			31.66	0.02	
Water	10.32			-	-	
Potassium iodide	1.43			108.35	0.15	
Water	10.32			-	-	
Acetonitrile		12.38		6.08	0.08	
Dichloromethane			295	11.16	3.29	
$MgSO_4$			2	54.24	0.08	
Distillation				-	-	
Phenylboronic acid	0.67			1,419.73	0.96	26.12
K_2CO_3	1.83			6.74	0.01	
$PdCl_2(PPh_3)_2$	0.06			16,701.40	0.93	
Water		2.38		-	-	
Dimethoxyethane		13.49		94.77	1.28	
Water			21	-	-	
Diethyl ether			159	22.89	3.63	
$MgSO_4$			2	54.24	0.08	
Heptane			284	4.59	1.30	
Ethyl acetate			160	3.63	0.58	
Silica gel			390	44.41	17.34	
9-Fluorenone	0.87			162.72	0.14	4.17
Magnesium	0.13			36.32	0.00	
Tetrahydrofuran		3.17		6.94	0.03	
Methanol			68	2.21	0.15	
Hydrochloric acid (5%)			19	3.13	0.06	
Methanol			68	2.21	0.15	
Acetic acid			90	40.12	3.63	

Continues on the next page

Continues from the previous page

Chemical name	Weight reagent (g/g)	Weight solvent (g/g)	Weight workup (g/g)	Price of Chemical ($/kg)	Material cost ($/g product)	Cost per step ($/step)
Iodic acid	0.92			371.09	0.34	1.61
Iodic acid	0.28			371.09	0.10	
Sulfuric acid		0.31		74.74	0.02	
Acetic acid		14		40.12	0.56	
Water		0.5		-	-	
Potassium hydroxide			0.14	21.21	0.00	
Water			1	-	-	
Toluene			71	4.08	0.29	
Toluene			71	4.08	0.29	
Potassium *t*-butoxide	1.05			1.05	0.16	27.52
$Pd(OAc)_2$	0.012			44,499.40	0.53	
$P(tBu)_3$	0.022			53,053.50	1.17	
Toluene		12		4.08	0.05	
Dichloromethane			201	11.16	2.24	
Na_2SO_4			1	12.79	0.01	
Ethyl acetate			2	3.63	0.01	
Dichloromethane			527	11.16	5.88	
Silica gel			263	66.41	17.47	
Total	**5.8**	**45.9**	**2399**	**-**	**-**	**91.67**

Table S10: Materials quantities and cost for the synthesis of Spiro-OMeTAD via route 2.

Chemical name	Weight reagent (g/g)	Weight solvent (g/g)	Weight workup (g/g)	Price of Chemical ($/kg)	Material cost ($/g product)	Cost per step ($/step)
1-iodoanisole	2.43			510.31	1.24	41.56
4-methoxyphenylamine	1.9			128.82	0.24	
CuI	0.2			115.74	0.02	
K2CO3	2.9			6.74	0.02	
L-proline	0.25			90.63	0.02	
DMSO		7		8.52	0.06	
ethyl acetate			252	3.63	0.91	
Na2SO4			1.9	12.79	0.02	
ethyl acetate			66	3.63	0.24	
petroleum ether			437	13.95	6.10	
silica gel			492	66.41	32.67	
2-Bromoanline	1.25			706.7	0.88	5.72
Hydrochloric acid	4.4			62.6	0.28	
Water	13			-	-	
$NaNO_2$	0.6			31.66	0.02	
Water	13			-	-	
Potassium iodide	1.8			108.35	0.20	
Water	13			-	-	
Acetonitrile		15.6		6.08	0.09	
Dichloromethane			372	11.16	4.15	
$MgSO_4$			1.9	54.24	0.10	
Distillation					-	
Phenylboronic acid	0.85			14,19.73	1.21	32.91
K_2CO_3	2.3			6.74	0.02	
$PdCl_2(PPh_3)_2$	0.07			16,701.4	1.17	
Water		3		-	-	
Dimethoxyethane		17		94.77	1.61	
Water			27	-	-	
Diethyl ether			200	22.89	4.58	
$MgSO_4$			1.9	54.24	0.10	
Heptane			358	4.59	1.64	
Ethyl acetate			201	3.63	0.73	
Silica gel			492	44.41	21.85	
9-Fluorenone	1.09			162.72	0.18	5.25
Magnesium	0.16			36.32	0.01	
Tetrahydrofuran		4		9.94	0.04	
Methanol			86	2.21	0.19	
Hydrochloric acid (5%)			24	3.13	0.08	
Methanol			86	2.21	0.19	
Acetic acid			114	40.12	4.57	

Continues on the next page

Continues from previous page

Chemical name	Weight reagent (g/g)	Weight solvent (g/g)	Weight workup (g/g)	Price of Chemical ($/kg)	Material cost ($/g product)	Cost per step ($/step)
Iron(III) chloride	0.002			17.09	0.00	0.73
Bromine	2			44.33	0.09	
Chloroform		11		2.6	0.03	
NH_4OH (25%)			4	8.14	0.03	
Chloroform			75	2.6	0.20	
Ethanol			40	9.53	0.38	
Sodium *t*-butoxide	1.05			277.30	0.29	22.26
$Pd_2(dba)_3$	0.066			1,6272	1.07	
$P(tBu)_3$	0.023			53,053.5	1.22	
Toluene		12		4.08	0.05	
Ethyl acetate			134	3.63	0.49	
$MgSO_4$			1	54.24	0.05	
Ethyl acetate			120	3.63	0.44	
Hexane			175	6.79	1.19	
Silica gel			263	66.41	17.47	
Total	**15.3**	**54**	**2654**	**-**	**-**	**108.43**

References

1 C. M. Cardona, W. Li, A. E. Kaifer, D. Stockdale and G. C. Bazan, *Adv. Mater.*, 2011, **23**, 2367–2371.

2 M. L. Petrus, *Azomethine-based Donor Materials for Organic Solar Cells*, Delft University of Technology, Delft, 2014.

3 G.-S. Liou and C.-W. Chang, *Macromolecules*, 2008, **41**, 1667–1674.

4 R. F. Nelson and R. N. Adams, *J. Am. Chem. Soc.*, 1966, **90**, 3925–3930.

5 M. L. Petrus, R. K. M. Bouwer, U. Lafont, S. Athanasopoulos, N. C. Greenham and T. J. Dingemans, *J. Mater. Chem. A*, 2014, **2**, 9474–9477.

6 H. Li, K. Fu, A. Hagfeldt, M. Grätzel, S. G. Mhaisalkar and A. C. Grimsdale, *Angew. Chemie - Int. Ed.*, 2014, **53**, 4085–4088.

7 T. Leijtens, I. Ding, T. Giovenzana, J. T. Bloking, M. D. Mcgehee and A. Sellinger, *ACS Nano*, 2012, **6**, 1455–1462.

8 D. Yang, Z. Yang, W. Qin, Y. Zhang, S. F. Liu and C. Li, *J. Mater. Chem. A*, 2015, DOI: 10.1039/C5TA01824B.

9 C. Olson, D. Veldman, K. Bakker and F. Lenzmann, *Int. J. Photoenergy*, 2011, **2011**, 1–11.

10 T. P. Osedach, T. L. Andrew and V. Bulović, *Energy Environ. Sci.*, 2013, **6**, 711–718.

11 *$1/W Photovoltaic Systems White Paper to Explore a Grand Challenge from Solar*, ARPA-E, Washington, DC, 2010.

12 C. Lambert, G. Nöll, E. Schmälzlin, K. Meerholz and C. Braeuchle, *Chem. - A Eur. J.*, 1998, **4**, 2129–2135.

13 J. H. Lin, A. Elangovan and T. I. Ho, *J. Org. Chem.*, 2005, **70**, 7397–7407.

14 C. Teng, X. Yang, C. Yang, S. Li, M. Cheng, A. Hagfeldt and L. Sun, *J. Phys. Chem. C*, 2010, **114**, 9101–9110.

15 M. Yano, Y. Ishida, K. Aoyama, M. Tatsumi, K. Sato, D. Shiomi, A. Ichimura and T. Takui, *Synth. Met.*, 2003, **137**, 1275–1276.

16 C.-W. Chang and G.-S. Liou, *J. Mater. Chem.*, 2008, **18**, 5638.

17 A. K. Mohanakrishnan, A. Hucke, M. A. Lyon, M. V. Lakshmikantham and M. P. Cava, *Tetrahedron*, 1999, **55**, 11745–11754.

18 S. H. Kim, J. Choi, C. Sakong, J. W. Namgoong, W. Lee, D. H. Kim, B. Kim, M. J. Ko and J. P. Kim, *Dye. Pigment.*, 2015, **113**, 390–401.

19 N. He, B. Li, H. Zhang, J. Hua and S. Jiang, *Synth. Met.*, 2012, **162**, 217–224.

20 C. Lambert, J. Schelter, T. Fiebig, D. Mank and A. Trifonov, *J. Am. Chem. Soc.*, 2005, **127**, 10600–10610.

21 J. Lv, Q. Liu, J. Tang, P. Perdih and K. Kranjc, *Tetrahedron*, 2012, **53**, 5248–5252.

22 K. Zhang, L. Wang, Y. Liang, S. Yang, J. Liang, F. Cheng and J. Chen, *Synth. Met.*, 2012, **162**, 490–496.

23 H. Zhang, H. Yi, G. Wang, B. Yang and S.-D. Yang, *Org. Lett.*, 2013, **15**, 6186–6189.

24 B. A. Kamino, B. Mills, C. Reali, M. J. Gretton, M. A. Brook and T. P. Bender, *J. Org. Chem.*, 2012, **77**, 1663–1674.

25 J. Karthikeyan, R. Haridharan and C. H. Cheng, *Angew. Chemie - Int. Ed.*, 2012, **51**, 12343–12347.

26 N. J. Jeon, J. H. Noh, Y. C. Kim, W. S. Yang, S. Ryu and S. Il Seok, *Nat. Mater.*, 2014, **13**, 897–903.